

## CRYSTAL STRUCTURE OF $^{154}\text{Sm}_{0.5}\text{Sr}_{0.5}\text{MnO}_3$ MANGANITE: A-TYPE ANTIFERROMAGNETIC PHASE AND FERROMAGNETIC POLARONS

A.I. Kurbakov<sup>1</sup>, V.A. Ryzhov<sup>1</sup>, A.V. Lazuta<sup>1</sup>, V.A. Trounov<sup>1</sup>,  
C. Martin<sup>2</sup>, A. Maignan<sup>2</sup>, M. Hervieu<sup>2</sup> and I.O. Troyanchuk<sup>3</sup>

<sup>1</sup>Petersburg Nuclear Physics Institute RAS, Gatchina, St. Petersburg, 188300 Russia

<sup>2</sup>Laboratoire CRISMAT, UMR 6508 ISMRA et Universite de Caen, 14050 Caen, France

<sup>3</sup>Institute of Physics of Solids and Semiconductors, NASB, ul. P. Brovki 17, 220072, Minsk, Belarus

$^{154}\text{Sm}_{0.6}\text{Sr}_{0.4}\text{MnO}_3$  investigated in Ref. [1] was used to prepare  $^{154}\text{Sm}_{0.5}\text{Sr}_{0.5}\text{MnO}_3$ . Mixed powder of the initial sample added with adequate amounts of  $\text{SrCO}_3$  and  $\text{MnO}_2$  was treated at 1270 K for 48 hours with a few intermediate grinding to complete decarbonation. The obtained powder was pressed into the form of pellets and a synthesis was carried out at 1470 K and then at 1770 K for 12 hours. After it, the sample was slowly cooled down to 1070 K with a rate of 5 K/min followed by a quenching performed down to room temperature. A cation composition was determined by an energy dispersive spectroscopy (EDS) analysis on an analyser mounted on the base of the three electron microscopes.

At room temperature the high resolution electron microscopy (HREM) reveals a strained and complex nanostructural state of *Pbnm* phase, which is generated by the co-existence of twinning domains, on the one hand, and the weak monoclinic distortions, on the other hand. All the images have been recorded using a weak electron current density, as soon as the crystal has been correctly oriented. The average size of the domains is a few ten nanometers. The multiple boundaries due to the small size of the twinning domains induce strain effects. At 92K, the [001] ED *Pbnm* patterns (Fig.1a) exhibit the weak extra satellites. These satellites are the well known signature of the charge ordering and can be associated to short range ordering (SRO) phenomena. The enlarged pattern (Fig.1b) shows that they stay in incommensurate positions. The relative intensity of the satellites with regard to the Bragg reflections of a *Pbnm*-type cell, despite hardly measurable, clearly varies from one crystal to the other, from visible (Fig.1a) to scarcely visible or absent.

The neutron diffraction data were analyzed with program FULLPROF. The nuclear structure is described by the orthorhombic *Pbnm* setting for  $T = 135 \text{ K} \div 300 \text{ K}$ . In agreement with the ED results, we added the *Ibmm* phase at the refinement. There are the common variable coordinates of the atomic positions in these space groups. It allows us to improve the fit factors. A volume fraction of the *Ibmm* phase is evaluated as  $\sim 3.4\%$  and is independent on temperature down to structural transition. At  $T = 300 \text{ K}$ , the cell parameters are:  $a = 5.4477(1) \text{ \AA}$ ,  $b = 5.4217(1) \text{ \AA}$ ,  $c/\sqrt{2} = 5.4046(2) \text{ \AA}$  and  $a = 5.4506(3) \text{ \AA}$ ,  $b = 5.4163(2) \text{ \AA}$ ,  $c/\sqrt{2} = 5.4223(3) \text{ \AA}$  for the *Pbnm* and for *Ibmm* structures, respectively.

The nuclear peaks for  $2\theta = 2 \text{ K} \div 135 \text{ K}$  can be only described by using two crystallographic phases. The structure can be considered as a mixture of the two *Pbnm* phases with the same atomic positions in the unit cell but with the different cell parameters. Amount of the high-temperature phase decreases whereas the second phase increases with decreasing temperature from 135 K down to 75 K. Below 75 K, when the full magnetic ordering is established, the ratio between both phases is stabilized. Fig.2c presents  $T$ -dependencies of the volume fractions. The main structural parameters obtained in the  $T$ -range  $1.5 \text{ K} \div 300 \text{ K}$  are displayed in Fig.2(a-e). It is seen that the unit cells of both phases are characterized by a relation  $a > b > c/\sqrt{2}$  (the  $O'$  structure) for all the temperatures. No  $T$ -hysteresis of the structural parameters is found in cooling and heating modes around 135 K in contrast to the results on  $\text{Sm}_{0.6}\text{Sr}_{0.4}\text{MnO}_3$  [1]. Fig.2(d, e) shows the Jahn-Teller (JT) distortion of the  $\text{MnO}_6$  octahedra. Above 135K, the Mn-O distances are close to each other. As it is seen, the apical distances in both phases found below 135K do not change with temperature.

Phase II is characterized by an apical compressed structure, whereas the apical distance is between the equatorial ones for phase I that is associated with a different character of their orbital ordering. The Mn-(O1,O2)-Mn angles are weakly changed with temperature. Their values practically coincide in both phases and are closed to the parameters at 1.5K: Mn-O1-Mn angle =  $161.5(5)^\circ$  and Mn-O2-Mn angle =  $166.5(5)^\circ$ .

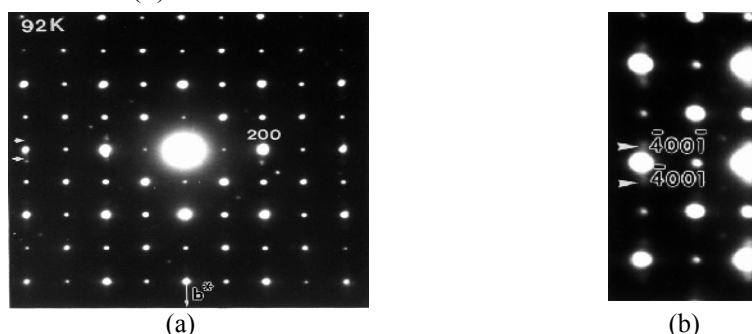


Fig.1. Panel (a) displays a typical [001] ED pattern recorded at 92K. The small white arrows show the satellites close to the  $(\bar{4}00)$  reflection of the **Pbnm** cell. Panel (b) exhibits the enlargement of a part of the ED pattern at 92K. The two satellites are indexed using four **hklm** indices.

An analysis of the magnetic contributions indicates that the ground state is a mixture of the two magnetic phases: F and AF-A. The F order certainly corresponds to the high temperature structure I, since the structural peaks belonging to the different structural phases are resolved, and the reflexes of phase I exhibit only the extra  $T$ -dependence related to the F contribution. The AF-A order forms at  $T_N \approx 135$  K. It can be identified with crystallographic phase II. As it usually occurs, the AF-A state develops in a structure with an orbital ordering taking place in the  $a$ - $b$  plane. However, the small angle AF reflexes have a larger width in the comparison with the structural ones (the resolution function of the diffractometer is taken into account). This can be due to either the existence of the two close unresolved peaks from the two AF-A states belonging to the phases II and I, or to an usual broadening related to finite size of the AF-A regions.

We can't determine whether the F ordering appears or not in a narrow temperature range just below  $T_{st}$ . The refinements with and without the F contribution ( $\leq 0.3\mu_B$ ) in the intensities of the corresponding nuclear peaks practically coincide for 135 K and 125 K. The reasons of this ambiguity are the complications of two structural and two magnetic phases, a limited number of the F peaks, and a reducing of the F phase at decreasing temperature that masks a relatively small F contribution near  $T_{st}$ . An additional problem in the determination of the  $M_F(T)$  is related to the presence of the *Ibmm* phase that gives contribution to the same structure reflexes as the F component. Its volume fraction (3.4%) and structure parameters are independent on temperature from room temperature down to  $T_{st}$ . These fixed values are used at the refinement for  $T \leq T_{st}$ . Thus, we present the  $M_F(T)$  data below 110 K. Note that the origination of the F state by a jump that starts at 130 K is found in the  $M_2$  measurements [2]. As the refinement of the neutron data shows, the F moment is aligned along the  $c$ -axis, whereas the AF moment is parallel to the  $b$ -axis. Non any traces of the AF-CE phase are observed over the whole temperature range.

We consider first the simplest magnetic structure when crystalline phases I and II exhibit F and AF-A ordering, respectively. It is strongly supported by the correspondence of the magnetic and orbital orders in the appropriate structural phases. Fig.2f shows the  $T$ -dependence of the F moment ( $M_F = 1.9(1) \mu_B/\text{Mn}$  at  $T = 1.5$  K). There is a reasonable correspondence between the volume fraction ( $V_{FI}$ ) and magnetization of the F phase and the bulk magnetization value obtained at 4.2K ( $1.5\mu_B / V_{FI} \approx 2.38 \mu_B/\text{Mn}$ , [2]). The metallic behavior of the sample can be attributed to the F phase since the AF-A phase is expected to be insulating. This is supported by the single crystal properties of this compound which suggest the AF insulating ground state [3,4]. In addition, a polycrystalline

$\text{Sm}_{0.45}\text{Sr}_{0.55}\text{MnO}_3$  also exhibits the homogeneous insulating ground state with the crystal and magnetic structures coinciding with those of phase II [5]. The small value of the F moment ( $M_F \approx 1.9 \mu_B/\text{Mn}$  at  $T = 1.5 \text{ K}$ ) suggests the presence of a magnetic disordering in the ground state. This phenomenon may be attributed to a spin-glass state that coexists with the F states. The spin-glass phase may be an intermediate one between the AF-A and F structures due to a competition of the F and AF couplings of the F-ordered  $ab$ -planes. A similar weakly ferromagnetic spin-glass state was observed in  $\text{Pr}_{1-x}\text{Ca}_x\text{MnO}_3$  at  $x = 0.3$  where this state coexisted with an AF-pseudo-CE phase [6,7]. As it is clear from Fig.2d, the F metallic state reveals the coherent JT effect similar to the phase separated  $\text{Sm}_{0.6}\text{Sr}_{0.4}\text{MnO}_3$  [1]. It is not a surprising result. In the phase separated  $\text{La}_{1-x}\text{Ca}_x\text{MnO}_3$  ( $x = 0.47, 0.5$ ; the  $Pbnm$  symmetry) the F phase also reveals these distortions whose magnitude and weak apical-compressed character are close to those of our compound [8].

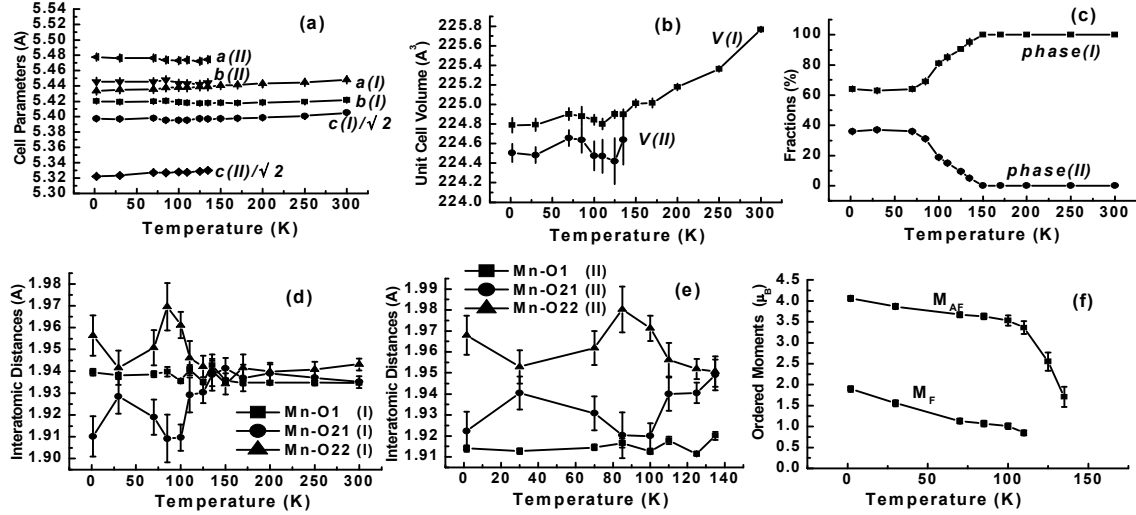


Fig.2. Temperature dependencies of the structural and magnetic parameters obtained from neutron diffraction data by the Rietveld refinement (the  $Pbnm$  symmetry). Panel (a) shows the  $T$ -dependencies of the lattice constants for the both crystalline phases. Panel (b) does the same for the unit cell volumes of these phases. Panel (c) displays the temperature variation of their volume fractions. Panels (d) and (e) present Mn-O bond lengths vs.  $T$  for the high-temperature (I) and low-temperature (II) structural phases, respectively. Panel (f) shows temperature evolutions of the F and AF magnetic moments. All the solid lines on these panels are a guide for the eyes.

The magnetic moment of the AF phase is found to be  $4.1(1) \mu_B/\text{Mn}$  at  $1.5 \text{ K}$ . As far as we know, it is the first observation of a so large Mn magnetic moment that contradicts the conventional picture where  $M_{AF} = 3.5 \mu_B/\text{Mn}$  for the formal  $\text{Mn}^{3+}$  and  $\text{Mn}^{4+}$  states. This new result corresponds to the theoretical prediction based on the unrestricted Hartree-Fock calculations [9]. The main peculiarity of this picture is that all the Mn ions are in  $d^4$ -state due to electron transfer from an oxygen  $\text{O}^{2-}$  ion to a neighboring  $\text{Mn}^{4+}$  ion, and formation of F-polarons consisting of the two Mn ions separated by the  $\text{O}^-$  ion. Magnetic moments of the Mn ions are approximately  $4 \mu_B$ , the moment of  $\text{O}^-$  is about  $-0.7 \mu_B$ , and the each polaron has a net moment closed to  $7 \mu_B$ . Formation of F-polarons is supported in some extent by the data on magnetization of the F domains in  $\text{La}_{0.5}\text{Ca}_{0.5}\text{MnO}_3$  with the phase separated ground state [10]. However, this approach predicts the AF-A ground state, so that our result is the more essential and obvious evidence in support of such electronic structure. It is remarkable, that all structural parameters of the AF-A phase for our manganite at  $T = 1.5 \text{ K}$  practically coincide with those of  $\text{Nd}_{0.5}\text{Sr}_{0.5}\text{MnO}_3$  with the AF-CE state at  $T = 10 \text{ K}$  (the  $Pbnm$  symmetry), besides  $a \approx 5.51 \text{ \AA}$  in the later [11]. This result agrees with an alternating ordering of  $d(3x^2-r^2)/d(3y^2-r^2)$  orbitals of the  $\text{Mn}^{3+}$  ions (the CE-type) as it is expected for the new AF-A state [9]. The evidence for the short range charge ordering obtained by the ED at  $92 \text{ K}$  refers certainly to this phase since it is the structure that can exhibit such an ordering. The similar phase separated ground state is found also in polycrystalline  $\text{La}_{0.5}\text{Ca}_{0.5}\text{MnO}_3$  with the two

crystal phases I' and II' closed to phases I and II of our compound. The phases I' and II' exhibit the F and AF-CE ordering, respectively [8].

As it is indicated above, the F order can only occur in phase I. At the same time, AF-A state associated with phase II may partially develop in phase I. Consequently, one can consider the case when phase I is described by a mixture of the F and AF-A states. The fit has been performed at 1.5K so that all structural and magnetic parameters have been varied independently at a fixed fraction of the AF-A phase in the structure I ( $V_{AFI}$ ). This model gives exactly the same structural parameters as the first variant with practically the same quality of the agreement between observed and calculated patterns for  $V_{AFI}=0-80\%$ . We get the following results for  $V_{AFI}=20\%$ :  $M_{AFI}=3.5(1)\mu_B/\text{Mn}$  and  $M_{FI}=2.90(7)\mu_B/\text{Mn}$ ;  $M_{AFII}=3.4(2)\mu_B/\text{Mn}$ . The  $V_{AFI}=20\%$  is the minimal volume fraction of the AF-A state that gives desirable  $M_{AFI}=3.5(1)\mu_B/\text{Mn}$ . The  $M_{AFI}$  increases with decreasing  $V_{AFI}$  and can become unrealistic large (for example,  $M_{AFI}\approx 4.7(1)\mu_B/\text{Mn}$  for  $V_{AFI}=15\%$ ). Although this refinement agrees with the data, it is unlikely to correspond to the real situation. The AF-A state is closely related to the definite type of the orbital ordering corresponding to phase II. Therefore, it is difficult to expect the appearance of the relatively large fraction of the saturated AF-A state in structure I that is appropriate for the F ordering. Thus this variant of the magnetic structure of phase I is less justified than the first one.

Another scenario is that phase I exhibits the homogeneous canted ground AF state. The corresponding refinement gives the same structural parameters for both phases as those of the two previous variants. At 1.5 K, the magnetic moments are found to be: F component =  $2.34(6)\mu_B/\text{Mn}$ , AF component =  $1.62(8)\mu_B/\text{Mn}$  for a moment of the phase I and  $M_{AFII}=3.4(1)\mu_B/\text{Mn}$ . Thus, we obtain the large dominating F component, small AF moment and, correspondingly, the unusual large canted angle. Canted AF state, however, may occur at a low doping ( $x\sim 0.1$ ) near a border between the AF and F insulating phases and it is characterized, in contrast to our case, by a comparable small F component. The findings on this matter were reported for  $\text{La}_{1-x}\text{Ca}_x\text{MnO}_3$  ( $x=0.05, 0.08$ ) [12]. As far as we know, the origin of the canted state just at  $x=0.5$  has not been observed or predicted so far. On the contrary, the coexistence (competition) of the F and AF phases, which form the heterogeneous magnetic states of the compound around  $x=0.5$ , was found in  $\text{La}_{0.5}\text{Ca}_{0.5}\text{MnO}_3$  [8,10]. It is significant that in the LaCa manganite the net F and AF-CE states coexisted in the charge ordered regions, non any traces of the canted state being found [10]. In our compound, the coexisting F metallic and AF-A insulating states correspond to the homogeneous ground states of the system at  $x=0.45$  (F metallic) [13] and  $x=0.55$  (AF-A insulating) [5], respectively. These reasons suggest that the canted state is very unlikely in the present case. This work was supported by joint Russian-Belorussian Foundation for Basic Research, Grants No 04-02-81051 RFBR-Bel2004\_a, F04R-076 and partly by the State Program of neutron investigation.

## References

- [1] I.D. Luzyanin, V.A. Ryzhov, D.Yu.Chernyshov, et al., Phys. Rev. B **64**, 094432 (2001).
- [2] see paper of V.A. Ryzhov, et al. “**Magnetic and transport...**” in this Proceeding.
- [3] Y. Tomioka, H. Kuwahara, A. Asamitsu et al., Appl. Phys. Lett. **70**, 3609 (1997).
- [4] V.Yu. Ivanov, A.A. Mukhin et al., J. Magn. Magn. Mater. **258 – 259**, 535 (2003).
- [5] A.I. Kurbakov, V.A. Trounov, C. Martin et al., Crystallography Reports **50**, 185 (2005).
- [6] C. Frontera, J. L. García-Munõz, A. Llobet, et al., Phys. Rev. B **62**, 3381 (2000).
- [7] P. G. Radaelli, R. M. Ibberson, D. N. Argyriou, et al., Phys. Rev. B **63**, 172419 (2001).
- [8] Q. Huang, J.W. Lynn, R.W. Erwin, et al., Phys. Rev. B **61**, 8895 (2000).
- [9] G. Zheng, C. H. Patterson, Phys. Rev. B **67**, R220404 (2003).
- [10] J.C. Loudon, N.D. Mathur, P.A. Midgley, Nature **420**, 797 (2002).
- [11] R. Kajimoto, H. Yoshizawa, H. Kawano, et al., Phys. Rev. B **60**, 9506 (1999).
- [12] F. Moussa, M. Hennion, G. Biotteau, et al., Phys. Rev. B **60**, 12299 (1999).
- [13] A.V. Lazuta, V.A. Ryzhov, A.I. Kurbakov, et al., J. Magn. Magn. Mater. **258-259**, 315 (2003).